Elsevier Editorial System(tm) for Ceramics International

Manuscript Draft

Manuscript Number: CERI-D-20-09073R1

Title: Phase stability and microstructure morphology of microwave-sintered magnesia-partially stabilised zirconia

Article Type: Full length article

Keywords: MgO-PSZ; phase stability; microstructure morphology; microwave heating

Corresponding Author: Professor guo chen,

Corresponding Author's Institution: yunnan minzu university

First Author: guo chen

Order of Authors: guo chen; Qiannan Li; Yeqing Ling; Hewen Zheng; Jin Chen; Qi Jiang; Kangqiang Li; Jinhui Peng; Mamdouh Omran; Lei Gao

Abstract: In this work, microwave heating approach was introduced into the preparation process of zirconia materials to overcome the tricky technical defects during the traditional electric arc furnace method. Magnesia-partially stabilised zirconia (MgO-PSZ) with enhanced stability and a uniform microstructure was prepared via microwave heating of a ZrO2 sample manufactured by the electric arc furnace method. The effects of microwave heating on the phase stability properties, microstructure, and surface morphology of the prepared MgO-PSZ sample were evaluated via X-ray diffraction (XRD), Raman spectroscopy, Fourier transform infrared (FT-IR) spectroscopy, and Scanning electron microscopy, and the obtained results suggested that the stability rate of the MgO-PSZ sample improved from the initial value of 81.19% to 94.82% after microwave heating at 1300 °C for 1 h. As a result of the martensitic conversion of ZrO2 material, the m-ZrO2 diffraction peaks were suppressed at the same time. Additionally, a similar changing trend was noticed in the XRD pattern, Raman spectrum, and FT-IR spectrum, indicating a decrease in the m-ZrO2 phase content in the microwave treated products. Furthermore, the microstructure on the surface of the microwave-sintered MgO-PSZ sample was improved in contrast to the raw MgO-PSZ sample, and became relatively more uniform and smooth. This study determined the optimal microwave heating conditions for the preparation of MgO-PSZ material with enhanced performance, and can provided as a good foundation for developing the further related research on zirconia materials preparing by microwave heating technology.

Phase stability and microstructure morphology of microwave-sintered magnesia-partially stabilised zirconia

Guo Chen [a, b], Qiannan Li [a], Yeqing Ling [a], Hewen Zheng [a], Jin Chen [a, b, **],

Qi Jiang [b, 1], Kangqiang Li [b, **], Jinhui Peng [a, b], Mamdouh Omran [c], Lei Gao [a, *]

[a] *Kunming Key Laboratory of Energy Materials Chemistry, Yunnan Minzu University, Kunming 650500, P.R. China.*

[b] *Faculty of Metallurgical and Energy Engineering, Kunming University of Science and Technology, Kunming 650093, P.R. China.*

[c] *Process Metallurgy Research Group, Faculty of Technology, University of Oulu, Finland.*

[*] Corresponding author: glkust2013@hotmail.com

[**] Co-Corresponding author: kqlikust@126.com, jinchen@kust.edu.cn

[1] The authors contributed equally to this work and should be regarded as co-first authors.

Abstract:

In this work, microwave heating approach was introduced into the preparation process of zirconia materials to overcome the tricky technical defects during the traditional electric arc furnace method. Magnesia-partially stabilised zirconia (MgO-PSZ) with enhanced stability and a uniform microstructure was prepared via microwave heating of a ZrO_2 sample manufactured by the electric arc furnace method. The effects of microwave heating on the

phase stability properties, microstructure, and surface morphology of the prepared MgO-PSZ sample were evaluated via X-ray diffraction (XRD), Raman spectroscopy, Fourier transform infrared (FT-IR) spectroscopy, and Scanning electron microscopy, and the obtained results suggested that the stability rate of the MgO-PSZ sample improved from the initial value of 81.19% to 94.82% after microwave heating at 1300 °C for 1 h. As a result of the martensitic conversion of ZrO_2 material, the m-ZrO_2 diffraction peaks were suppressed at the same time. Additionally, a similar changing trend was noticed in the XRD pattern, Raman spectrum, and FT-IR spectrum, indicating a decrease in the m-ZrO_2 phase content in the microwave treated products. Furthermore, the microstructure on the surface of the microwave-sintered MgO-PSZ sample was improved in contrast to the raw MgO-PSZ sample, and became relatively more uniform and smooth. This study determined the optimal microwave heating conditions for the preparation of MgO-PSZ material with enhanced performance, and can provided as a good foundation for developing the further related research on zirconia materials preparing by microwave heating technology.

Keywords: MgO-PSZ; phase stability; microstructure morphology; microwave heating

1 Introduction

Zirconia (ZrO_2) is a high-performance material with advantages including high-temperature resistance, corrosion resistance, and high hardness. As a high-grade and high-quality refractory material, ZrO_2 plays an important role in applications including sizing nozzles, skateboard bricks, fused cast bricks, and hollow balls [1–3]. In addition, ZrO_2-based materials are commonly applied in high-tech areas such as bioceramics, electronic ceramics,

functional ceramics, and structural ceramics [4–6]. For applications involving heating or cooling processes, the crystalline structure of ZrO_2 usually undergoes a martensitic transformation, resulting in the co-existence of concomitant crystalline structures of ZrO_2 at different temperatures [7, 8]. Specifically, the main phase of pure ZrO_2 at room temperature is monoclinic-ZrO_2 (m-ZrO_2); at a temperature of 1170 °C, the m-ZrO_2 phase begins to convert into a tetragonal-ZrO_2 (t-ZrO_2) phase, and the t-ZrO_2 phase transforms into a cubic-ZrO_2 (c-ZrO_2) phase at a temperature exceeding 2370 °C [9, 10]. However, the transformation between the three crystal structures of ZrO_2 is usually accompanied by shear strain and volume changes, leading to the catastrophic destruction of the structure of pure ZrO_2 materials [11]. During a heating–cooling cycle, the metastable t-ZrO_2 phase in pure ZrO_2 is easily transformed into a stable m-ZrO_2 phase, accompanied by a volume expansion of 3%–5%. This volume effect is prone to create cracks, which decreases the thermal shock resistance of the material and thus further limits the application of ZrO_2 in the field of high-temperature processes [12].

To stabilise the structure of ZrO_2 materials, cations with a radius greater than that of Zr^{4+} are introduced into ZrO_2 lattices to replace some of the Zr^{4+} lattice point positions by doping oxides into pure ZrO_2 materials; meanwhile, replacement solid solutions are formed in these ZrO_2 materials by doping, which maintains the stable phase structure of the resultant doped ZrO_2 materials at room temperature, thereby achieving a toughening effect for pure ZrO_2 materials [13, 14] and leading to the formation of partially stabilised zirconia (PSZ) materials. The commonly used stabilizers include CaO [15], MgO [16], Y_2O_3 [17], and Ce_2O_3 [18]. Currently, partially stabilised zirconia materials are mainly prepared through the electric arc

furnace method from fully stabilised zirconia (FSZ). However, this preparation process has several issues including large energy consumption, long operation time, high processing temperature, and high production cost [14]. To solve these issues, microwave heating technology was introduced into the preparation of PSZ materials in this study.

Microwave heating is an important technical approach for preparing high-performance novel materials and for modifying traditional materials [19–22]. The possibility of applying microwave heating technology to the materials preparation is based on the possession of decent dielectric properties by the preprocessed materials [23–25], which causes the internal molecular vibrations of ZrO_2 under the action of microwave energy, further leading to the formation of more-optimised PSZ materials compared with the traditional electric arc furnace method [26]. Guo et al. [26] reported that the microwave-absorbing ability of fused ZrO_2 was decent, and the temperature of fused ZrO_2 increased to 1475 °C within 4 min. Mazageri [27] used microwave heating to prepare 8 mol% yttrium oxide-stabilised zirconia, and highlighted that the microwave-heated samples possessed a more uniform microstructure and optimized grain size. Li et al. [28] prepared CaO-PSZ from natural oblique zircon by microwave heating at 1300 °C for 80 min; moreover, the obtained PSZ product consisted of fine and uniform particles, with the bending strength reaching 138.271 MPa. Compared with traditional heating treatment technology, ZrO_2 material prepared via microwave heating presents unparalleled advantages, such as a shorter reaction time, faster heating rate, smaller particle size, uniformly distributed microstructure, few by-products produced, and environmental-friendly production [29–32].

The tradition preparation process of partially stabilised zirconia materials through the

electric arc furnace method are plagued with several issues such as high processing temperature, long operation time, large energy consumption, and high production cost [14]. Meanwhile, the recent studies have elucidated the alternative applications of microwave heating to replace conventional heating on the preparation of ZrO_2 materials doped with CaO stabilizer, and highlighted that microwave technology presents excellent effects on the microstructure characteristics and phase stability properties of CaO-ZrO_2 materials, with prominent advantages including shorter process time and lower process temperature [2, 10]. However, no report has involved with the laboratory-scale experiments focusing on the optimization preparation of magnesia partially stabilized zirconia (MgO-PSZ) using microwave heating approach. Therefore, in this study, magnesia-PSZ (MgO-PSZ) material with enhanced stability and a uniform microstructure was optimally prepared via microwave heating at a temperature of 1300 °C for 1 h from ZrO_2 sample prepared by electric arc furnace melting. The effects of microwave heating on the microstructure, phase stability, and surface morphology of the prepared MgO-PSZ material were elucidated by X-ray diffraction (XRD), scanning electron microscopy (SEM), Raman spectroscopy, and Fourier transform infrared (FT-IR) spectroscopy.

2 Materials and methods

2.1 Materials

The as-received raw ZrO_2 sample was smelted by an electric arc furnace in a factory in Zhengzhou, Henan Province, P.R. China. The results of chemical composition analysis of the as-received ZrO_2 sample were provided by an affiliated analysis institution. It can be observed

from Table 1 that ZrO_2 is the main component of the as-received sample, which accounts for 92.4% of the sample. Meanwhile, there are traces of MgO, SiO_2, Al_2O_3, Fe_2O_3, and TiO_2 in the sample, wherein a content of 4.0% of magnesium oxide (MgO) can be noticed.

The XRD pattern of the as-received ZrO_2 sample is depicted in Fig. 1. Moreover, the peaks in this XRD pattern were identified by referring to the standard cards of c-ZrO_2 (JCPDS: 49-1642), m-ZrO_2 (JCPDS: 37-1484), and t-ZrO_2 (JCPDS: 42-1164). As can be seen in Fig. 1, the diffraction peaks of m-ZrO_2 appear at $2\theta = 28.29°$ and $2\theta = 31.58°$, and the diffraction peak of c-ZrO_2 appears at $2\theta = 35.08°$, confirming that the raw ZrO_2 sample contained m-ZrO_2 and c-ZrO_2 phases; meanwhile, the main diffraction peaks of t-ZrO_2 appear at $2\theta = 30.18°$, $2\theta = 35.15°$, and $2\theta = 50.40°$. However, the diffraction peaks of t-ZrO_2 overlap with those of c-ZrO_2, indicating that the existence of t-ZrO_2 in the raw ZrO_2 sample is uncertain. Moreover, the diffraction peaks of a separate MgO phase are absent in the as-received sample, indicating that all of the MgO components enter the lattice nodes of ZrO_2 and form a stable replacement solid solution structure with ZrO_2. In summary, it was concluded that the as-received ZrO_2 sample was the MgO-PSZ material.

2.2 Instrumentation and procedure

The application of microwave heating was expected to improve the performance and stability of the MgO-PSZ material. Microwave heating experiments for MgO-PSZ materials were conducted in a microwave heating furnace (RWS-6, WYWAVE), which the microwave furnace was manufactured by the Key Laboratory of Unconventional Metallurgy of Ministry of Education attached to Kunming University of Science and Technology (Kunming City, Yunnan Province, P.R. China). The schematic of the equipment is demonstrated in Fig. 2. The

components of the microwave furnace included a microwave energy feeding system, a microwave cavity, a water-cooling system, a heat preservation system, a crucible, an exhaust system, a computer control system, and an infrared thermometer.

Before microwave heating, the as-received sample was placed in a drying oven (DHG9079A, Shanghai Yiheng Scientific Instrument Co., Ltd) and subjected to drying at 105 °C for 12 h. Subsequently, 50.0 g of the dried sample was weighed and equally distributed into 5 parts using an electronic balance (CP114, Shanghai Ohaus Instrument Co., Ltd). Afterwards, the five divided samples, each with a mass of 10.0 g, were introduced into the microwave furnace and processed at heating temperatures of 900 °C, 1000 °C, 1100 °C, 1200 °C and 1300 °C, with a holding time of 1 h and a microwave power constant of 3 kW. After completing the heating experiments, the heated samples were naturally cooled and collected for subsequent analysis, wherein the analysis of phase stability properties was expected to yield the optimal heating temperature. Therefore, by controlling the heating temperature at an optimal parameter value, the effects of holding time on the stability of the MgO-PSZ sample were investigated; moreover, different holding times of 1 h, 2 h, 3 h, and 4 h were employed. In a manner similar to that followed in the case of the heating experiments, the insulated samples were naturally cooled and collected after reaching the specific holding time.

2.3 Characterisation

The phase transitions of the raw MgO-PSZ sample (i.e., the as-received ZrO_2 sample) and the microwave-heated MgO-PSZ sample were investigated using an X-ray diffractometer (D8 ADVANCE A25×, Bruker, Germany), wherein Cu target Ka-ray (λ=1.54056 Å) was used

as the target source, the tube voltage was 40 kV, and the tube current was 20 mA; moreover, the samples were scanned in the θ-2θ step-scan mode at a scan rate of 5°/min in the range of 10°–100°. The chemical structures of the raw and microwave-heated MgO-PSZ samples were characterised using a confocal Raman spectrometer (InVia, Renishaw, UK), equipped with an Ar^+ laser in the spectral scattering detection range of 100 cm^{-1}–800 cm^{-1}. The surface functional groups of the raw and microwave-heated MgO-PSZ samples were determined using an FT-IR spectrometer (NICOLET-IS10, USA). FT-IR experiments of MgO-PSZ samples were performed using pure potassium bromide (KBr) mixed with the samples at a ratio of 100:1 and in the scanning spectral range of 4000 cm^{-1}–500 cm^{-1}. The microstructures of the raw and microwave-heated MgO-PSZ samples were analysed using a field-emission scanning electron microscope (XL30 ESEM-TM, Philips, Netherlands), with the acceleration voltage and resolution set at 30 kV and 3 nm, respectively.

3 Results and discussion

3.1 Phase stability properties analysis

The phase stability properties of ZrO_2 materials are commonly determined by calculating their stability rates. Additionally, the superiority of the microwave heating approach can be evaluated by comparing the phase stability properties of the raw and microwave-heated MgO-PSZ samples. The stability rates of the raw and microwave-heated MgO-PSZ samples were calculated using the following equation [33, 34]:

$$\text{Stability rate} = \frac{\text{Intensity of } 29.92°}{\text{Intensity of } 28.06° + \text{Intensity of } 31.24° + \text{Intensity of } 29.92°} \times 100\% \quad (1)$$

where intensity of 29.92° denotes the intensity of c-ZrO_2 diffraction peak, and intensities of

28.06° and 31.24° indicate the intensities of m-ZrO_2 diffraction peaks. Thus, the stability rate of the raw MgO-PSZ sample was 81.19%, as calculated using Eq. (1). The effects of microwave heating temperature and holding time on the phase stability properties of MgO-PSZ ceramics were explored, and are depicted in Fig. 3.

The effects of heating temperature on the phase stability properties of the microwave-heated MgO-PSZ samples that were processed under a holding time of 1 h are depicted in Fig. 3(a). As shown in Fig. 3(a), the phase stability properties of the MgO-PSZ samples significantly improved with the introduction of microwave heating. Specifically, after microwave treatment at 900 °C for 1 h, the stability rate of the MgO-PSZ sample improved from the initial value of 81.19% to 83.01%; furthermore, the stability rate improved from 83.01% to 94.82% with an increase in the heating temperature from 900 °C to 1300 °C, and the peak of the stability rate appeared at 1300 °C. Therefore, based on Eq. (1), it can be surmised that the increase in heating temperature promoted the progress of the martensitic transformation of ZrO_2 materials, and thus led to a gradual phase change and corresponding grain growth [7, 8]. With an increase in treatment temperature, the m-ZrO_2 content gradually decreased and transformed into t-ZrO_2; thereby, the phase structure of the microwave-heated MgO-PSZ sample remained stable under normal temperature [9, 10]. Moreover, it can be observed from Fig. 3(a) that the stability rate improved from 94.61% to 94.82% with an increase in the heating temperature from 1200 °C to 1300 °C, with a slight increment of the stability rate. Therefore, it could be speculated that the continue increase of temperature (higher than 1300 °C) is unbeneficial to improve the stability rate; on the contrary, it may cause a decrease. In summary, the optimal heating temperature was determined at 1300 °C.

The effects of holding time on the phase stability properties of the microwave-heated MgO-PSZ samples that were processed at a constant microwave treatment temperature of 1300 °C are depicted in Fig. 3(b). As shown in Fig. 3(b), the stability rate of the microwave-heated MgO-PSZ sample exhibited a volatile trend with an increase in the holding time, which manifested as a change of the stability rate. The stability rate firstly decreased, subsequently increased, and finally decreased. The extension of the holding time under the same heating temperature led to an increase in the extent of the phase change in the MgO-PSZ sample, which further caused a fluctuation in the stability rate. For the experimental groups with holding times of 1 h and 2 h, the stability rates were 94.82% and 93.72%, respectively. Similarly, for the experimental groups with holding times of 3 h and 4 h, the stability rates were 94.50% and 91.06%, respectively. This variation in stability rates across the experimental groups with different holding times was mainly ascribed to the transformation of t-ZrO_2 into m-ZrO_2, which resulted from the extension of the holding time caused a decrease in both the content of the stable phase and the stability rate [9, 10]. Accordingly, it was found that the stability rate improved from 93.72% at 2 h to 94.50% at 3 h. Moreover, it can be inferred that these two effects act simultaneously, which in turn leads to fluctuations in the stability rates of the microwave-heated MgO-PSZ samples. From the above analysis, the optimal holding time was determined to be 1 h.

At present, partially stabilised zirconia (PSZ) materials in the industrial production mainly adopt the electric melting method, which has disadvantages such as high process temperature (above 1400 °C), long processing time (about 17 h), high consumption of carrier materials, and difficult equipment maintenance [35]. Regarding the related reports on the

traditional preparation of MgO-PSZ materials, Jiang et al. investigated the structure and mechanical properties of magnesia partially stabilized zirconia during cyclic heating and cooling from room temperature to 1450 °C, and found that increasing heating temperature promoted the increase of the phase stability properties and bending strength of MgO-PSZ [36]; besides, Guo et al. prepared 3.5 wt% magnesia partially stabilized zirconia (Mg-PSZ) refractory with an optimized sintering temperature of 1670 °C [37], and Li et al. have prepared CaO-doped partially stabilized zirconia with a heating temperature of 1450 °C and a holding time of 4 h [15]. Hence, compared with those traditional preparation experiments of MgO-PSZ materials, the advantages of microwave-sintered were prominent, such as the holding time decreased by 3 h and the heating temperature decreased by 150 °C.

3.2 XRD characterisation and analysis

By exploring the effects of holding time and heating temperature on the phase stability properties of the MgO-PSZ samples, the optimised preparation parameters of the MgO-PSZ sample via microwave heating were obtained, with a microwave heating temperature of 1300 °C and a holding time of 1 h. Based on the optimised parameters, the effects of microwave heating on the phase transitions of the MgO-PSZ sample were determined via XRD characterisation.

The XRD pattern of the MgO-PSZ sample optimally prepared via microwave heating at 1300 °C for 1 h is illustrated in Fig. 4. As depicted in Fig. 4, the phase composition of this microwave-heated MgO-PSZ sample was a mixture of three crystal phases, namely c-ZrO_2, m-ZrO_2, and t-ZrO_2. In the mixture, the dominant component was the c-ZrO_2 phase, and the minor component was the m-ZrO_2 phase; moreover, the corresponding stability rate was

94.82%. Compared with the raw MgO-PSZ sample (Fig. 1), the c-ZrO_2 diffraction peaks at 2θ = 30.12°, 2θ = 35.08°, and 2θ = 50.40° were stronger in the case of the microwave-heated MgO-PSZ sample. Additionally, the diffraction peaks for m-ZrO_2 phase at 2θ = 28.29° and 2θ = 31.58° became weaker, and the t-ZrO_2 phase was detected in the microwave-heated MgO-PSZ sample, which was attributed to the decreased content of m-ZrO_2. Therefore, it was inferred that the heating temperature of 1300 °C was favourable for the conversion of m-ZrO_2 to t-ZrO_2 [7, 8]. The remaining m-ZrO_2 included two parts: one part was the remaining m-ZrO_2 that failed to transform into t-ZrO_2, and the other part was m-ZrO_2 that formed by the reversible martensitic conversion of t-ZrO_2 to m-ZrO_2 during the cooling process.

3.3 Raman characterisation and analysis

The Raman spectra of the raw MgO-PSZ sample and microwave-heated MgO-PSZ sample are presented in Fig. 5. In the case of the raw MgO-PSZ sample, Raman vibration characteristic peaks were observed at 285.2 cm^{-1}, 319.2 cm^{-1}, 374.8 cm^{-1}, and 403.5 cm^{-1} (see Fig. 5(a)). Among these Raman peaks, the Raman peak at 285.2 cm^{-1} and 319.2 cm^{-1} were caused by the E_g vibration of t-ZrO_2; moreover, the Raman peaks at 374.8 cm^{-1} and 403.5 cm^{-1} resulted from the B_g vibration of m-ZrO_2. Therefore, based on the XRD and Raman analyses results (Fig. 1 and Fig. 5(a)) obtained for the raw MgO-PSZ sample, all three crystal structures were found to be present in the raw MgO-PSZ sample, namely m-ZrO_2, t-ZrO_2, and c-ZrO_2.

In the case of the MgO-PSZ sample optimally prepared via microwave treatment at 1300 °C for 1 h, four Raman peaks appeared at 285.8 cm^{-1}, 319.2 cm^{-1}, 355.8 cm^{-1} and 376.5 cm^{-1} (see Fig. 5(b)). The Raman peak at 285.8 cm^{-1} and 319.2 cm^{-1} were ascribed to the E_g

vibration of t-ZrO_2; moreover, the Raman peaks at 355.8 cm^{-1} and 376.5 cm^{-1} were caused by the B_g vibration of m-ZrO_2. Further, based on the Raman analysis results obtained for the raw MgO-PSZ sample and microwave-heated MgO-PSZ sample (Fig. 5(a) and Fig. 5(b)), it was found that the peak intensity of m-ZrO_2 was weak in the case of the microwave-heated MgO-PSZ sample, and the peak intensity of t-ZrO_2 decreased. This indicated that the m-ZrO_2 phase in the sample transformed into the t-ZrO_2 phase at 1300 °C, which resulted in an improvement in the stability rate of the MgO-PSZ sample.

3.4 FT-IR characterisation and analysis

The FT-IR spectra of the raw MgO-PSZ sample and microwave-heated MgO-PSZ sample are illustrated in Fig. 6. In the case of the raw MgO-PSZ sample (Fig. 6(a)), five characteristic FT-IR peaks appeared at 545.50 cm^{-1}, 1013.39 cm^{-1}, 1416.46 cm^{-1}, 1643.53 cm^{-1}, and 3447.56 cm^{-1}. Among these FT-IR peaks, the peak located at 545.50 cm^{-1} resulted from the contraction vibrations of Zr-O bonds, that peak at 1013.39 cm^{-1} was assigned to the bending vibrations of O-H bonds, and that at 1416.46 cm^{-1} was caused by the adsorbed CO_2 from air. Additionally, the characteristic peaks at 1643.53 cm^{-1} and 3447.56 cm^{-1} were ascribed to the bending vibrations of H-O-H bonds and the contraction vibrations of O-H bonds on the sample surface, respectively. In agreement with the XRD and Raman analysis, the contraction vibrations of the Zr-O bonds appeared in the FT-IR spectrum, which resulted from the infrared vibrations caused by the three crystal structures of ZrO_2.

In the case of the MgO-PSZ sample optimally prepared via microwave heating at 1300 °C for 1 h, the infrared vibration peaks appeared at 513.26 cm^{-1}, 1067.37 cm^{-1}, 1399.48 cm^{-1}, 1617.24 cm^{-1}, and 3447.47 cm^{-1} (Fig. 6(b)). The characteristic peak located at 1399.48

cm^{-1} was caused by the adsorbed CO_2 from air, which corresponded to the assignment of raw characteristic peak at 1416.46 cm^{-1}. The characteristic peak located at 1067.37 cm^{-1} was assigned to the bending vibrations of O-H bonds, which corresponded to the assignment of raw characteristic peak at 1013.39 cm^{-1}. Based on comparison with the raw characteristic peak at 1643.53 cm^{-1}, it was inferred that the peak at 1617.24 cm^{-1} was caused by the bending vibrations of H-O-H bonds. The characteristic peak at 3447.47 cm^{-1} was caused by the contraction vibrations of O-H bonds on the sample surface. Furthermore, the peak at 513.26 cm^{-1} was assigned to the contraction vibrations of Zr-O bonds. Based on a comparison with the characteristic peak at 545.50 cm^{-1} in the case of the raw MgO-PSZ sample, it was found the characteristic peak assigned to the contraction vibrations of Zr-O bonds shifted to a lower wavenumber (513.26 cm^{-1}) in the case of the microwave-heated MgO-PSZ sample, which indicated a red shift. The red shift was attributed to the martensitic transformation of ZrO_2 caused by the temperature change during the microwave heating process. The martensite transformation under the heating temperature (1300 °C) mainly manifested as a transformation from m-ZrO_2 to t-ZrO_2, which led to the enhancement in the phase stability of the MgO-PSZ sample.

3.5 SEM characterisation and analysis

The microstructures of the raw MgO-PSZ sample and the MgO-PSZ samples optimally prepared via microwave heating were compared by SEM characterisation; and the corresponding microstructures are shown in the SEM images in Fig. 7. For the raw MgO-PSZ sample (Figs. 7(a) and 7(b)), the particle shape was irregular; moreover, both the particle size and particle structure were uniform. For the MgO-PSZ sample optimally prepared via

microwave heating, the edges of the crystalline grains became smooth, and the clumping effect appeared between grains. In addition, the grains piled up and overlapped each other, which caused some grains to appear abnormally large, as observed from Fig. 7(c). Moreover, the surface of the microwave-heated MgO-PSZ sample became relatively smooth in contrast to the raw MgO-PSZ sample, with fine grains and few pores on the surface, as displayed in Fig. 7(d). Furthermore, the grain size was relatively more uniform, which indicated that microwave heating promoted the mutual fusion of the ZrO_2 grains with MgO acting as a stabiliser, contributing to the improvement in the phase stability of the MgO-PSZ sample.

4 Conclusions

In this study, microwave heating mean was applied to prepare MgO-PSZ materials instead of the traditional electric melting method, and the phase stability, microstructure, and surface morphology of MgO-PSZ material prepared by microwave heating were systematically investigated. The aim of this study was to optimise the preparation process of a MgO-PSZ sample. The results indicated that under microwave treatment at a heating temperature of 1300 °C for 1 h, the stability rate of the MgO-PSZ sample improved sharply from 81.19% to 94.82%. An increase in the microwave heating temperature contributed to the improvement in the stability of the MgO-PSZ sample. XRD and Raman analyses synchronously revealed a considerable increase in the t-ZrO_2 content and a significant decrease in the m-ZrO_2 content, which resulted from the martensitic conversion of ZrO_2 material with temperature change. Moreover, the martensitic conversion also caused a red shift related to the infrared vibration peak resulting from the contraction vibration of Zr-O

bonds. Additionally, the microwave-heated MgO-PSZ sample presented a smoother surface and more uniformly distributed microstructure compared with the raw MgO-PSZ sample, indicating that microwave heating promoted the mutual fusion of the ZrO_2 grains with MgO acting as a stabiliser, which further lead to uniform microstructure and enhanced phase stability of MgO-PSZ material. The introduction of microwave heating approach efficiently improved the tricky technical defects during the traditional electric arc furnace method, manifested by the heating temperature decreased by 150 °C, the holding time decreased by 3 h, and more uniform microstructure and enhanced stability properties. This work can provided a sound reference for the extended applications of microwave heating technology to the zirconia materials doped with various stabiliser.

Acknowledgments

The authors would like to acknowledge the National Natural Science Foundation of China (Grant No. 51764052) and the Innovative Research Team (in Science and Technology) in the University of Yunnan province for the financial support.

References

1. C. Patapy, F. Gouraud, M. Huger, R. Guinebretière, B. Ouladiaff, D. Chateigner, T. Chotard, Investigation by neutron diffraction of texture induced by the cooling process of zirconia refractories, J. Eur. Ceram. Soc. 34(15) (2014) 4043-4052. https://doi.org/10.1016/j.jeurceramsoc.2014.05.027.
2. K.Q. Li, Q. Jiang, J. Chen, J.H. Peng, X.P. Li, S. Koppala, M. Omran, G. Chen, The controlled preparation and stability mechanism of partially stabilised zirconia by

microwave intensification, Ceram. Int. 46(6) (2020) 7523-7530. https://doi.org/10.1016/j.ceramint.2019.11.251.

3. D.K. Leung, C.J. Chan, M. Rühle, F.F. Lange, Metastable crystallization, phase partitioning, and grain growth of ZrO_2-Gd_2O_3 materials processed from liquid precursors, J. Am. Ceram. Soc. 74(11) (2005) 2786-2792. https://doi.org/10.1111/j.1151-2916.1991.tb06844.x.
4. G. Chen, Y.Q. Ling, Q.N. Li, H.W. Zheng, K.Q. Li, Q. Jiang, J. Chen, M. Orman, L. Gao, Crystal structure and thermomechanical properties of CaO-PSZ ceramics synthesised from fused ZrO_2, Ceram. Int. 46(10) (2020) 15357-15363. https://doi.org/10.1016/j.ceramint.2020.03.079.
5. F. A. Kroger, Electronic conductivity of calcia-stabilized zirconia, J. Am. Ceram. Soc. 49(4) (2010) 215-218. https://doi.org/10.1111/j.1151-2916.1966.tb13237.x.
6. A.K. Pandey, K. Biswas, Influence of heating parameters on tribological properties of ceria stabilized zirconia bio-ceramics, Ceram. Int. 37(1) (2011) 257-264. https://doi.org/10.1016/j.ceramint.2010.08.041.
7. X.M. Zeng, A. Lai, C.L. Gan, C.A. Schuh, Crystal orientation dependence of the stress-induced martensitic transformation in zirconia-based shape memory ceramics, Acta. Mater. 116 (2016) 124-135. https://doi.org/10.1016/j.actamat.2016.06.030.
8. M. Mamivand, M.A. Zaeem, H.E. Kadiri, Effect of variant strain accommodation on the three-dimensional microstructure formation during martensitic transformation: Application to zirconia, Acta. Mater. 87 (2015) 45-55. https://doi.org/10.1016/j.actamat.2014.12.036.
9. S. Guo, Y. Kagawa, Isothermal and cycle properties of EB-PVD yttria-partially-stabilised zirconia thermal barrier coatings at 1150 and 1300 °C, Ceram. Int. 33(3) (2007) 373-378. https://doi.org/10.1016/j.ceramint.2005.10.005.

10. G. Chen, Y.Q. Ling, Q.N. Li, H.W. Zheng, K.Q. Li, Q. Jiang, L. Gao, M. Orman, J.H. Peng, J. Chen, Stability properties and structural characteristics of CaO-partially stabilized zirconia ceramics synthesized from fused ZrO_2 by microwave heating, Ceram. Int. 46(10) (2020) 16842-16848. https://doi.org/10.1016/j.ceramint.2020.03.261.
11. P.E. Reyes-Morel, I.W. Chen, Transformation plasticity of CeO_2-stabilized tetragonal zirconia polycrystals: I, stress assistance and autocatalysis, J. Am. Ceram. Soc. 71(5) (2010) 343-353. https://doi.org/10.1111/j.1151-2916.1988.tb05052.x.
12. L.L. Fehrenbacher, L.A. Jacobson, Metallographic observation of the monoclinic-tetragonal phase transformation in ZrO_2, J. Am. Ceram. Soc. 48(3) (2010) 157-161. https://doi.org/10.1111/j.1151-2916.1965.tb16054.x.
13. A. Bogicevic, C. Wolverton, G.M. Crosbie, E.B. Stechel, Defect ordering in aliovalently doped cubic zirconia from first principles. Phys. Rev. B. 64(1) (2001) 014106. https://doi.org/10.1103/PhysRevB.64.014106.
14. R.C. Garvie, Structure and thermomechanical properties of partially stabilized zirconia in the CaO-ZrO_2 system, J. Am. Ceram. Soc. 55 (2010) 152-157. https://doi.org/10.1007/978-94-009-0741-6_15.
15. K.Q. Li, J. Chen, J.H. Peng, S. Koppala, M. Omran, G. Chen, One-step preparation of CaO-doped partially stabilized zirconia from fused Zirconia, Ceram. Int. 46(5) (2020) 6484-6490. https://doi.org/10.1016/j.ceramint.2019.11.129.
16. M.W. Yan, Y. Li, G.X. Yin, S.H. Tong, J.H. Chen, Synthesis and characterization of a MgO-$MgAl_2O_4$-ZrO_2, composite with a continuous network microstructure, Ceram. Int. 43(8) (2017) 5914-5919. https://doi.org/10.1016/j.ceramint.2017.01.082.
17. L.Q. Kong, S.Y. Zhu, Q.L. Bi, Z.H. Qiao, J. Yang, W.M. Liu, Friction and wear behavior of self-lubricating $ZrO_2(Y_2O_3)$-CaF_2-Mo-graphite composite from 20°C to 1000°

C, Ceram. Int. 40(7) (2014) 10787-10792. https://doi.org/10.1016/j.ceramint.2014.03.068.

18. Y.J. Xia, J.L. Song, D.N. Yuan, X.N. Guo, X. Guo, Synthesis and characterization of one-dimensional metal oxides: TiO_2, CeO_2, Y_2O_3-stabilized ZrO_2 and $SrTiO_3$, Ceram. Int. 41(1) (2015) 533-545. https://doi.org/10.1016/j.ceramint.2014.08.102.
19. K.Q. Li, J. Chen, G. Chen, J.H. Peng, R. Ruan, C. Srinivasakannan, Microwave dielectric properties and thermochemical characteristics of the mixtures of walnut shell and manganese ore, Bioresource. Technol. 286 (2019) 121381. https://doi.org/10.1016/j.biortech.2019.121381.
20. G. Chen, K.Q. Li, Q. Jiang, X.P. Li, J.H. Peng, M. Omran, J. Chen, Microstructure and enhanced volume density properties of FeMn78C8.0 alloy prepared via a cleaner microwave sintering approach, J. Clean. Prod. 262 (2020) 121364. https://doi.org/10.1016/j.jclepro.2020.121364.
21. K.Q. Li, J. Chen, J.H. Peng, R. Ruan, C. Srinivasakannan, G. Chen, Pilot-scale study on enhanced carbothermal reduction of low-grade pyrolusite using microwave heating, Powder. Technol. 360 (2020) 7523-7530. https://doi.org/10.1016/j.powtec.2019.11.015.
22. K.N. Sasi, G. Denys, P. Pascaline, J.A. Babu, Microwave mode of heating in the preparation of porous carbon materials for adsorption and energy storage applications-An overview, Renew. Sust. Energ. Rev. 124 (2020) 109743. https://doi.org/10.1016/j.rser.2020.109743.
23. K.Q. Li, G. Chen, X.T. Li, J.H. Peng, R. Ruan, M. Omran, J. Chen, High-temperature dielectric properties and pyrolysis reduction characteristics of different biomass-pyrolusite mixtures in microwave field, Bioresource. Technol. 294 (2019) 122217. https://doi.org/10.1016/j.biortech.2019.122217.

24. K.Q. Li, Q. Jiang, L. Gao, J. Chen, J.H. Peng, S. Koppala, M. Omran, G. Chen, Investigations on the microwave absorption properties and thermal behavior of vanadium slag: Improvement in microwave oxidation roasting for recycling vanadium and chromium, J. Hazard. Mater. 395 (2020) 122698. https://doi.org/10.1016/j.jhazmat.2020.122698.

25. K.Q. Li, J. Chen, J.H. Peng, R. Ruan, M. Orman, G. Chen, Dielectric properties and thermal behavior of electrolytic manganese anode mud in microwave field, J. Hazard. Mater. 381 (2020) 121227. https://doi.org/10.1016/j.jhazmat.2019.121227.

26. S.H. Guo, G. Chen, J.H. Peng, J. Chen, J.L. Mao, D.B. Li, L.J. Liu, Preparation of partially stabilized zirconia from fused zirconia using heating, J. Alloy. Compd. 506 (1) (2010) L5-L7. https://doi.org/10.1016/j.jallcom.2010.06.156.

27. M. Mazaheri, A.M. Zahedi, M.M. Hejazi. Processing of nanocrystalline 8 mol% yttria-stabilized zirconia by conventional, microwave-assisted and two-step heating, Mat. Sci. Eng. A-struct. 492(1) (2008) 261-267. https://doi.org/10.1016/j.msea.2008.03.023.

28. J. Li, J.H. Peng, S.H. Guo, W.W. Qv, W. Li, L.B. Zhang, G. Chen, Thermodynamic calculations of t to m martenstic transformation of ZrO_2-CaO binary system, Ceram. Int. 38 (4) (2012) 2743-2747. https://doi.org/10.1016/j.ceramint.2011.11.043.

29. A.A.B. Hamra, H.N. Lim, N.M. Huang, N.S.K. Gowthaman, H. Nakajima, M. Mahbubur Rahman, Microwave exfoliated graphene-based materials for flexible solid-state supercapacitor, J. Mol. Struct. 1220 (2020) 128710. https://doi.org/10.1016/j.molstruc.2020.128710.

30. K.Q. Li, G. Chen, J. Chen, J.H. Peng, R. Ruan, C. Srinivasakannan, Microwave pyrolysis of walnut shell for reduction process of low-grade pyrolusite, Bioresource. Technol. 291 (2019) 121838. https://doi.org/10.1016/j.biortech.2019.121838.

31. K.Q. Li, J. Chen, J.H. Peng, M. Omran, G. Chen, Efficient improvement for dissociation behavior and thermal decomposition of manganese ore by microwave calcination, J. Clean. Prod. 260 (2020) 121074. https://doi.org/10.1016/j.jclepro.2020.121074.

32. M. Fu, Z.T. Zhu, Z.H. Zhang, Q.R. Zhuang, W. Chen, Q.Y. Liu, Microwave deposition synthesis of $Ni(OH)_2$/sorghum stalk biomass carbon electrode materials for supercapacitors, J. Alloy. Compd. 846 (2020) 156376. https://doi.org/10.1016/j.jallcom.2020.156376.

33. Y. Murase, E. Kato, K. Daimon, Stability of ZrO_2 phases in ultrafine ZrO_2-Al_2O_3 mixtures, J. Am. Ceram. Soc. 69(2) (1986) 83-87. https://doi.org/10.1111/j.1151-2916.1986.tb04706.x.

34. M.Y. Zhang, L. Gao, J.X. Kang, J. Pu, J.H. Peng, M. Omran, G. Chen, Stability optimisation of CaO-doped partially stabilised zirconia by microwave heating, Ceram. Int. 45(17) (2019) 23278-23282. https://doi.org/10.1016/j.ceramint.2019.08.024.

35. A. Keyvani, M. Bahamirian, B. Esmaeili, Sol-gel synthesis and characterization of ZrO_2-25wt.%CeO_2-2.5wt.%Y_2O_3 (CYSZ) nanoparticles. Ceram. Int. 46(13) (2020) 21284-21291. https://doi.org/ 10.1016/j.ceramint.2020.05.219.

36. L. Jiang, S.Q. Guo, M.R. Qiao, M. Zhang, W.Z. Ding, Study on the structure and mechanical properties of magnesia partially stabilized zirconia during cyclic heating and cooling. Mater. Lett. 194 (2017) 26-29. https://doi.org/10.1016/j.matlet.2017.01.135.

37. L. Jiang, S.Q. Guo, Y.Y. Bian, M. Zhang, W.Z. Ding, Effect of sintering temperature on mechanical properties of magnesia partially stabilized zirconia refractory. Ceram. Int. 42(9) (2016) 10593-10598. https://doi.org/10.1016/j.ceramint.2016.03.136.

Table captions

Table 1 Chemical composition of the as-received raw zirconia sample

Figure captions

Fig. 1 XRD pattern of the as-received raw zirconia sample.

Fig. 2 Schematic of microwave heating furnace.

Fig. 3 Effects of (a) heating temperature and (b) holding time on the stability properties of MgO-PSZ samples.

Fig. 4 XRD pattern of the microwave-heated MgO-PSZ sample at 1300 °C for 1 h.

Fig. 5 Raman spectra of (a) the raw MgO-PSZ sample and (b) the microwave-heated MgO-PSZ sample at 1300 °C for 1 h.

Fig. 6 FT-IR spectra of (a) the raw MgO-PSZ sample and (b) the microwave-heated MgO-PSZ sample at 1300 °C for 1 h.

Fig. 7 SEM images of the MgO-PSZ samples before and after microwave heating; (a) the raw sample, 5000×; (b) 5000×; (c) the microwave-heated sample at 1300 °C for 1 h, 5000×; (d) 10000×.

Table 1 Chemical composition of the as-received raw zirconia sample

Composition	ZrO_2	MgO	SiO_2	Al_2O_3	TiO_2	Fe_2O_3
Mass/W%	92.4	4.0	2.3	1.0	0.2	0.1

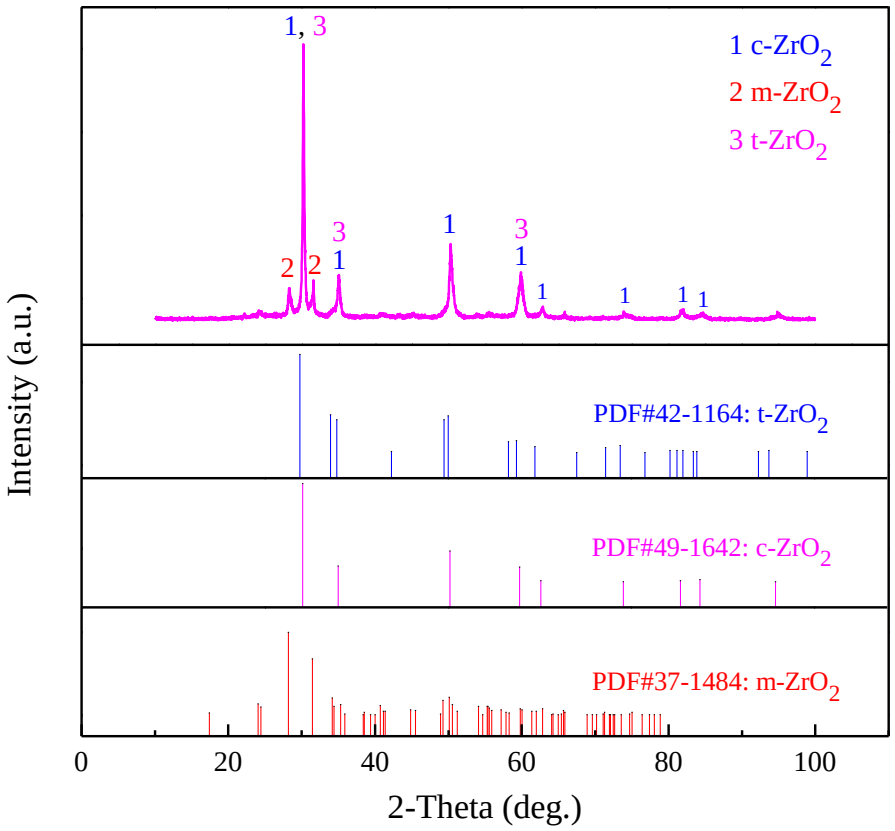

Fig. 1 XRD pattern of the as-received raw zirconia sample.

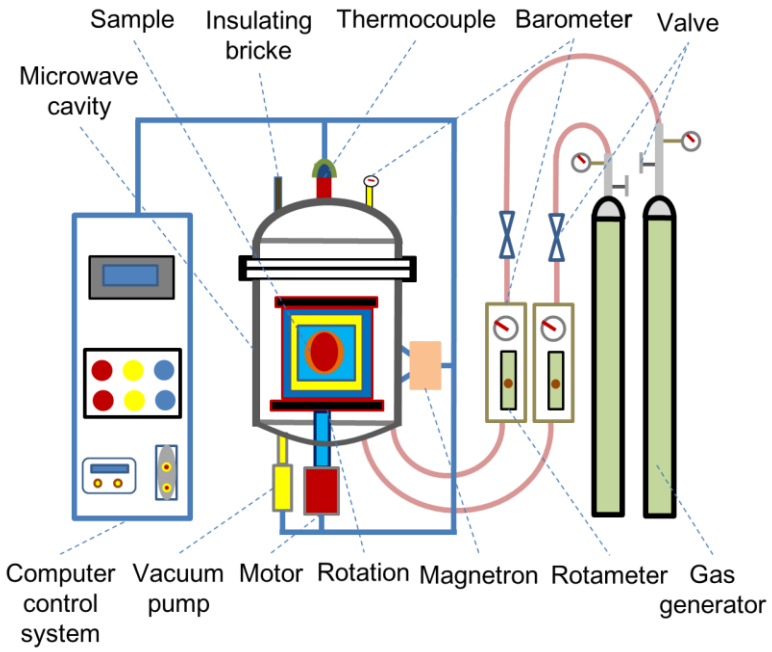

Fig. 2 Schematic of microwave heating furnace.

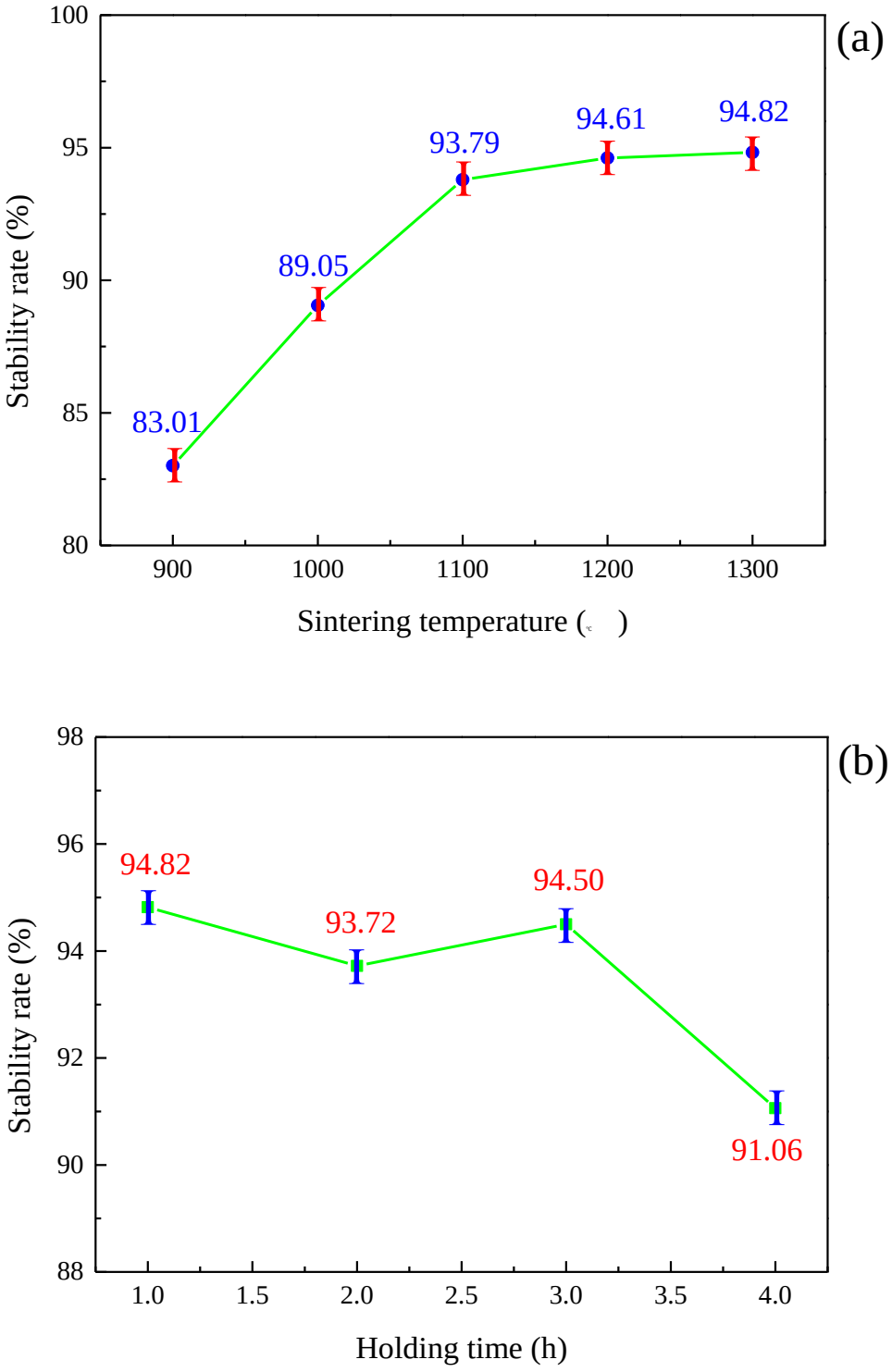

Fig. 3 Effects of (a) heating temperature and (b) holding time on the stability properties of MgO-PSZ samples.

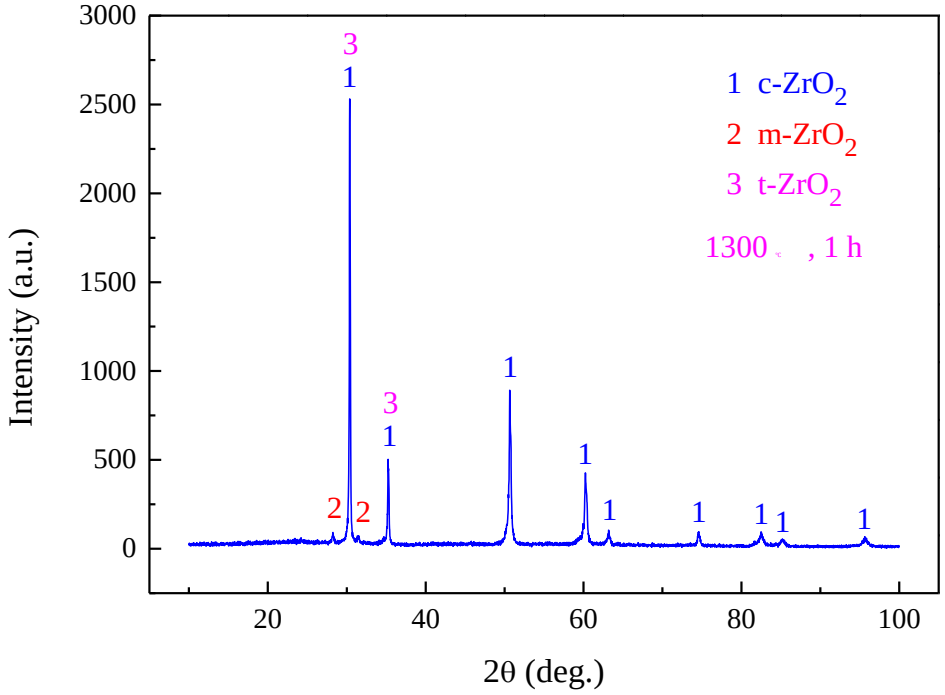

Fig. 4 XRD pattern of the microwave-heated MgO-PSZ sample at 1300 °C for 1 h.

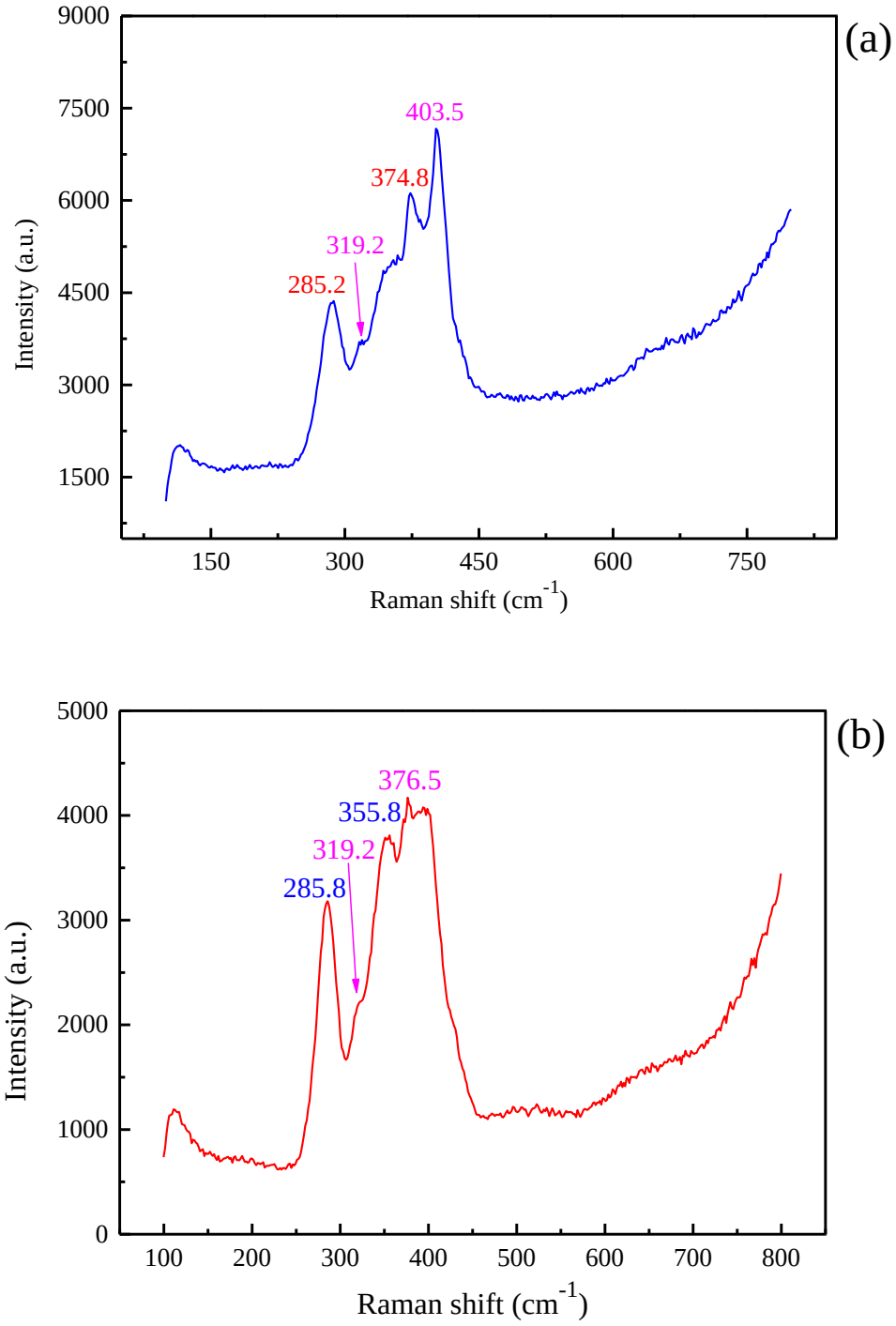

Fig. 5 Raman spectra of (a) the raw MgO-PSZ sample and (b) the microwave sintered sample at 1300 °C for 1 h.

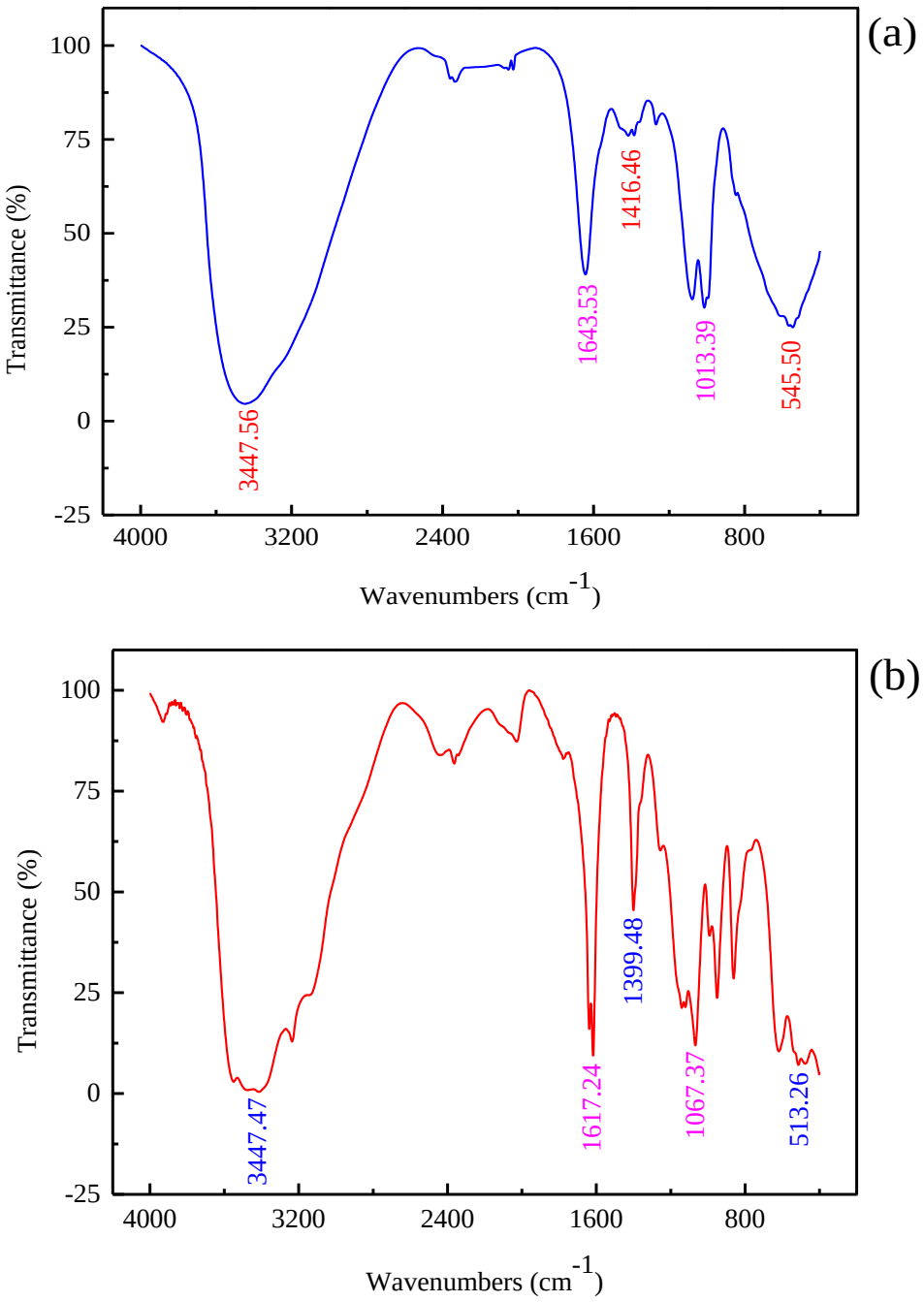

Fig. 6 FT-IR spectra of (a) the raw MgO-PSZ sample and (b) the microwave sintered sample at 1300 °C for 1 h.

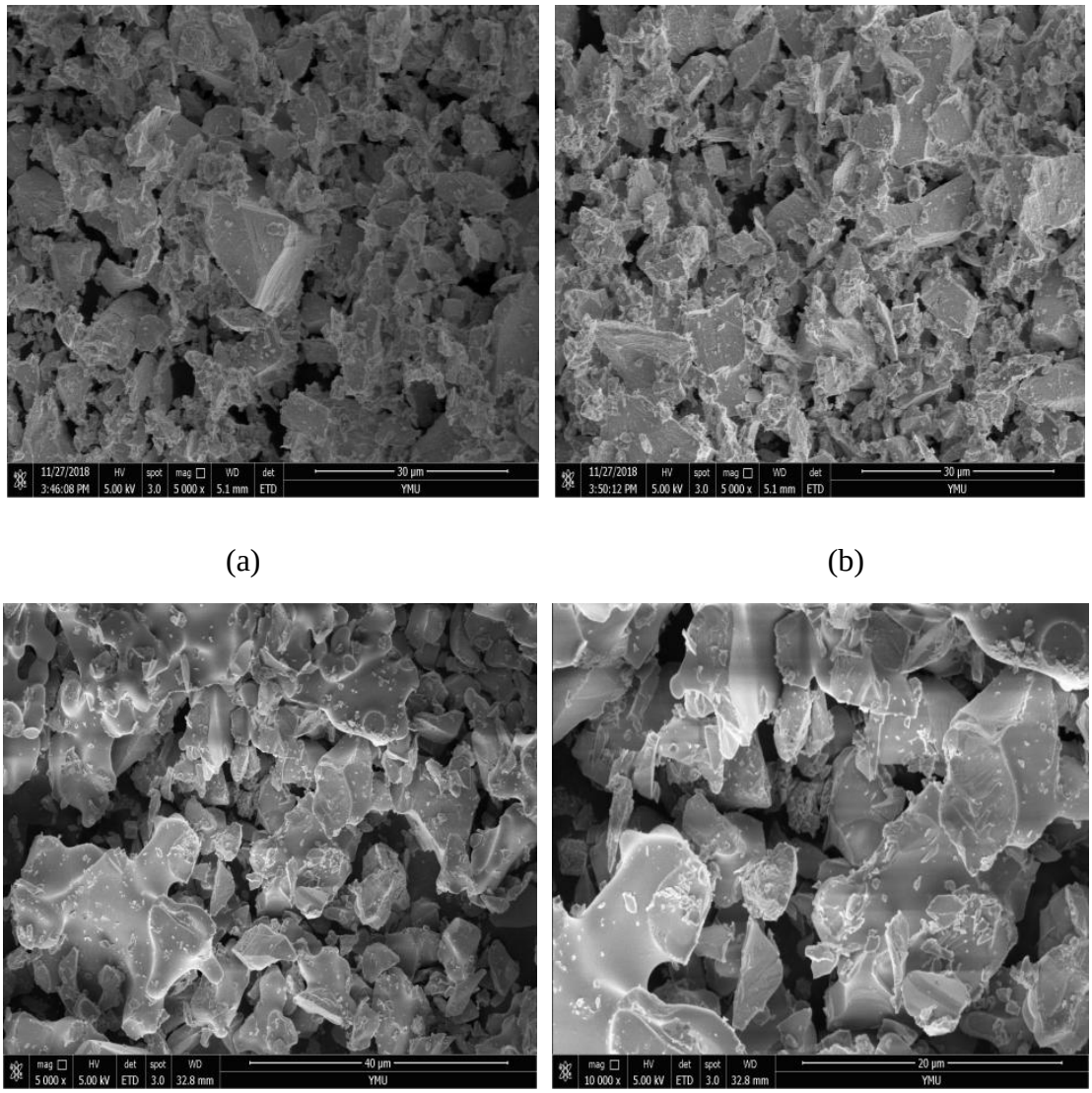

(a) (b)

(c) (d)

Fig. 7 SEM images of the MgO-PSZ samples before and after microwave heating; (a) the raw sample, 5000×; (b) 5000×; (c) the microwave-heated sample at 1300 °C for 1 h, 5000×; (d) 10000×.

***Declaration of Interest Statement**

Declaration of interests

☒ The authors declare that they have no known competing financial interests or personal relationships that could have appeared to influence the work reported in this paper.

☐The authors declare the following financial interests/personal relationships which may be considered as potential competing interests:

e-component

Click here to download e-component: Certificate-2020.8.10.pdf